ISSN 1070-3632, Russian Journal of General Chemistry, 2013, Vol. 83, No. 12, pp. 2438–2446. © Pleiades Publishing, Ltd., 2013.

Synthesis of Several New Lanthanide Glimepiride Complexes for Evaluation of Microbial Activity[1]

M. G. Abd El-Wahed[a], Samy M. El-Megharbel[a,b], Mohamed Y. El-Sayed[a], Yasmin M. Zahran[a], and Moamen S. Refat[b,c]

[a] *Department of Chemistry, Faculty of Science, Zagazig University, Egypt*
e-mail: msrefat@yahoo.com

[b] *Department of Chemistry, Faculty of Science, Taif University, 888 Taif, Kingdom Saudi Arabia*

[c] *Department of Chemistry, Faculty of Science, Port Said, Port Said University, Egypt*

Received October 7, 2013

Abstract—The complexation between lanthanide metal ions like Nd(III), Tb(III), and Er(III) with Glimepiride produces 1 : 1 molar ratio (metal : Glimepiride) monodentate complexes of general formula: $[M(GMP)(H_2O)_4]Cl_3 \cdot xH_2O$, where: M = Nd, Tb, and Er, x = 1, 10, respectively. The structures of obtained compounds were assigned by IR, ^{1}H NMR and UV/Vis spectra. Themogravimetric analysis and kinetic thermodynamic parameters have proved the thermal stability of Glimepiride complexes. Obtained lanthanide complexes showed significant effect against some bacteria and fungi.

DOI: 10.1134/S1070363213120402

INTRODUCTION

It has been reported that metal complexes may be more biologically active and less toxic as compared to the free ligand [1, 2]. In other words, many drugs exhibit modified pharmacological properties when administrated in the form of metallic complexes. Glimepiride, a sulfonylurea (SU) derivative, has been used in the treatment of type 2 diabetic patients in Europe and Asia. It has a mild effect on insulin secretion, with a hypoglycemic effect equivalent to that of glibenclamide [3]. Therefore, this new SU is anticipated to have additional extrapancreatic effects. Experiments have demonstrated that glimepiride activates insulin-mediated glycogen synthesis, inhibits hepatic gluconeogenesis and enhances glucose uptake [4, 5]. Many clinical studies support the data from animal models indicating that glimepiride can reduce insulin resistance [6–8]. However, the mechanism of this specific action has not been explained [9, 10]. The chemical formula of glimepiride is 3-ethyl-4-methyl-*N*-(4-[*N*-((1*r*,4*r*)-4-methylcyclohexylcarbamoyl)-sulfamoyl]phenethyl)-2-oxo-2,5-dihydro-1*H*-pyrrole-1-carboxamide [11] or 1-{[*p*-[2-(3-ethyl-4-methyl-2-oxo-3-pyrroline-1carboxamido) ethyl]phenyl]sulfonyl}-3-(*trans*-4-methylcyclohexyl)urea (Fig. 1).

It is a hypoglycemic drug which is potent in the treatment of non-insulin dependent diabetes mellitus (NIDDM) [12, 13]. Glimepiride is a white or off white crystalline powder, relatively insoluble in water, but its predicted water solubility is 1.6 mg/mL) that causes large variations in its bioavailability [14]. Metal complexes of Mn(II) and Co(II) have been synthesized with Glimeperide. The elemental analyses of the ligand as well as metal complexes indicate that complexes have 2 : 1 stoichiometry of the type $(C_{24}H_{34}N_4O_5S)_2M \cdot 2H_2O$, where M = Mn(II) or Co(II). The complexes have been characterized by their IR and electronic spectra and molar conductivity. Infrared spectral studies confirmed the coordination of sulphonyl oxygen on one side and enolic oxygen attached from other side of the metal ion. On the basis of electronic spectral values the complexes are proposed to have octahedral geometry. The data on molar conductivity also revealed that these complexes are non-ionic [15].

EXPERIMENTAL

All chemicals used were of the purest laboratory grade (Merck). Glimepiride (GMP) was a gift from Egyptian International Pharmaceutical Industrial Company (EIPICo). Carbon and hydrogen contents were determined using a Perkin-Elmer CHN 2400 device. Metal content was found gravimetrically by converting the compounds into their corresponding

[1] The text was submitted by the authors in English.

Table 1. Elemental analysis and physical data of Glimepiride and its complexes

Comp. no.	M_w	Color	Elemental analysis data (calculated/found)					Specific conductivity, Ω^{-1} cm^{-1} mol^{-1}
			C, %	H, %	N, %	Cl, %	M, %	
I	Off white	830.5	34.67/34.26	5.29/5.59	5.29/5.59	12.82/12.44	17.33/17.31	340
II	Yellow	845.5	34.06/34.40	5.20/5.52	5.20/5.52	12.59/12.65	18.80/18.90	213
III	Pink	1015.5	25.72/25.56	4.49/4.92	4.49/4.92	10.87/10.90	17.04/17.34	548

Table 2. Main IR data of Glimepiride and its metal complexes

Compound	ν(NH)	ν(C=O)	ν(S=O)	ν(M–O)	ν(SO_2N)	ν(H_2O)
Glimepiride	3288	1706	1394	–	1155	–
I	3287	1706	1348	682	1153	3055
II	–	1704	1404	681	1126	3042
III	–	1705	1404	656	–	3041

oxides. IR spectra were recorded on a Bruker FTIR Spectrophotometer (4000–400 cm^{-1}) in KBr pellets. UV-vis spectra were done in DMSO solvent with concentration of (1.0×10^{-3} M) for Glimepiride and its complexes on an Jenway 6405 spectrophotometer with 1 cm quartz cell, in the range of 800–200 nm. Molar conductivities of freshly prepared 1.0×10^{-3} mol dm^{-3} DMSO solutions were measured using Jenway 4010 conductivity meter. ^{1}H NMR spectra were recorded on a Varian Gemini 200 MHz spectrometer using DMSO-d_6 as solvent. Thermogravimetric analysis (TGA and DTG) were carried out in dynamic nitrogen atmosphere (30 mL/min) with a heating rate of 10°C/min using Schimadzu TGA-50H thermal analyzer.

[Nd(GMP)(H_2O)$_4$]Cl_3·H_2O complex (I). Glimepiride (0.17 g, 1.0 mmol) was added to 15 mL of methanol and pH was adjusted to 8.4. Then 10 mL of methanolic solution of (0.13 g, 1.0 mmol) of $NdCl_3$ was added with continuously stirring, after that the mixture was warmed at about ~60°C and then neutralized. Precipitate that formed immediately, was filtered off, washed several times with minimum amount of hot methanol and dried under vacuo over anhydrous $CaCl_2$.

[Tb(GMP)(H_2O)$_4$]Cl_3·H_2O (II). Similar procedure was used to prepare Tb(III) complex. Reaction mixture was allowed to stay at room temperature for about 1 h with constant stirring and then heated on a water bath at ~60°C for 30 min. The white complex was filtered off, washed several times with hot methanol and dried under vacuum over anhydrous $CaCl_2$.

[Er(GMP)(H_2O)$_4$]Cl_3·$10H_2O$ (III). The Er(III) glimepiride complex was prepared by the same method used for preparation of Nd(III) complex.

Antimicrobial activity test. The hole well method, as described in [17], was used. The investigated isolates of bacteria were seeded in tubes with nutrient broth (NB). The seeded NB (1 cm^3) was homogenized in the tubes with 9 cm^3 of melted (45°C) nutrient agar (NA). The homogeneous suspensions were poured into Petri dishes. The holes (4 mm in diameter) were done in the cooled medium. Tested solutions, 0.2 mL, were applied in a hole using a micropipette. After incubation for 24 h in a thermostat at 25–27°C, the inhibition (sterile) zone diameters (including disk) were measured. An inhibition zone diameter of over 7 mm indicates that the tested compound is active against the bacteria under investigation. Complexes were tested against *E. coli* (G–), *Bacillus subtilis* (G+), *Aspergillus nigar* and *Penicillium*.

RESULTS AND DISCUSSIONS

Elemental analysis (CHN) data agrees quite well with the proposed structure of the colored Glimepiride complexes (Table 1). Prepared substances are thermally stable above > 250°C, soluble in DMSO and DMF. Conductivity values for all three complexes, measured in DMSO at room temperature, fall in the range typical for electrolytes [18].

Infrared spectral studies. IR spectra [19–33] of the ligand and the isolated complexes were recorded in the range of 4000–450 cm^{-1} and the probable assignments are given in Table 2. The proposed

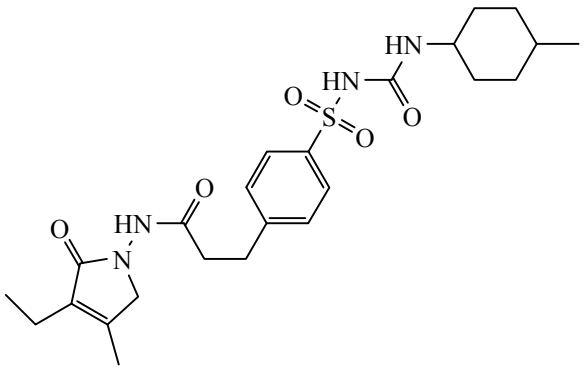

Fig. 1. Glimepiride (GMP).

structure for the isolated complexes supported by IR absorption bands and characterized by the absorption of carbonyl (C=O) group at 1706, 1704, and 1705 cm^{-1} in Nd(III), Tb(III), and Er(III) ligand complex, respectively. Also the NH group observed at 3288 cm^{-1} in the glimepiride ligand, shifted to 3287 cm^{-1}. In Tb–Glimepiride and Er–Glimepiride complexes the band is just disappear. The next IR band of structural significance of the ligand appears at 1394 cm^{-1} which may be assigned to ν(S=O) which got shifted downward at 1348 cm^{-1} in Nd–Glimepiride complex while in Tb–Glimepiride and Er–Glimepiride complexes it just appear at 1404 cm^{-1}, respectively. The shift of the ν(C=O) and ν(S=O) to decreased frequencies in the complexes indicate that these groups are involved in the complexation. The linkage through amide–O and sulphone–O atom was further supported by the appearance of a band in the far IR region at 682, 681, and 656 cm^{-1}, in the Nd(III), Tb(III), and Er(III) complex that may be assignable to M–O frequency [24]. Additional band in the complex region of Nd(III) at 1443 cm^{-1} compared with IR spectra of free ligand has tentatively been assigned to six membered enolic ring structure modified to chelate ring formation in complex [25–28]. A strong band in the region of 3055, 3042, and 3041 cm^{-1} indicates presence of coordinated water for Nd, Tb, and Er-glimepiride complexes, respectively.

Table 3. Electronic spectral data of the Glimepiride metal complexes

Comp. no.	λ_{max}, nm	ε, $mol^{-1}\,cm^{-1}$	Assignment
I	270	520	*n*–π* (*trans*)
	232	627	*n*–π* (*trans*)
	780	33	π–π* (*trans*)
	386	42	π–π* (*trans*)
	252	408	*n*–π* (*trans*)
	215	426	*n*–π* (*trans*)
II	270	686	*n*–π* (*trans*)
	259	857	*n*–π* (*trans*)
	225	963	*n*–π* (*trans*)
	783	35	π–π* (*trans*)
	264	40	π–π* (*trans*)
	247	384	*n*–π* (*trans*)
III	270	508	*n*–π* (*trans*)
	258	598	*n*–π* (*trans*)
	251	636	*n*–π* (*trans*)
	781	33	π–π* (*trans*)
	373	49	π–π* (*trans*)
	264	274	π–π* (*trans*)
	256	496	*n*–π* (*trans*)
	227	482	*n*–π* (*trans*)

UV-vis Spectra. UV-Vis spectra of Glimepiride and its complexes in DMSO exhibit peaks, listed in Table 3. There are two absorption maxima peaks at ranges of 33–49 nm and 202–636 nm, assigned to π–π* and *n*–π* transitions within Glimepiride metal complexes. The electronic absorption spectra of all Glimepiride complexes show a bathochromic shift for π–π* transitions, rather than for *n*–π* ones. This shift is attributed to the complexation and the change in the electronic configuration of the complexes formed. Electronic spectrum of Nd(III)–Glimepiride complex shows a weak absorption peak in the visible region probably due to spin-orbit forbidden transitions.

^{1}H NMR Spectra. The ^{1}H NMR spectra present the persuasive confirmation of the coordination modes. Thus, the ^{1}H NMR spectra of complexes (Fig. 2) on comparing with those of spectrum of the free Glimepiride indicate that, Glimepiride ligand acts as bidentate ligand through the phenolic OH group and carboxylic OH group. The data obtained are in agreement with the suggested coordination through the carboxylic and phenolic groups by observing the absence of the signals of two protons that appear in the free ligand about δ = 11.00 and 5.00 ppm, respectively and due to different chemical environments the signals of aromatic protons at 6.00–8.00 ppm, observed with decreasing intensities.

Thermogravimetric analysis. The thermal decomposition curves (TG/DTG and DTA) are shown in Fig. 3, while TG weight loss data, DTG and DTA peak temperatures are listed in Table 4. The thermal decomposition of $[Nd(GMP)(H_2O)_4]Cl_3{\cdot}H_2O$ (**I**) complex occurs in six steps. The first degradation occurs at 298–346 K, being assigned to elimination of one water molecule (weight loss: observed, 2.0% and calculated, 2.1%). The second step occurs at 498 K being is

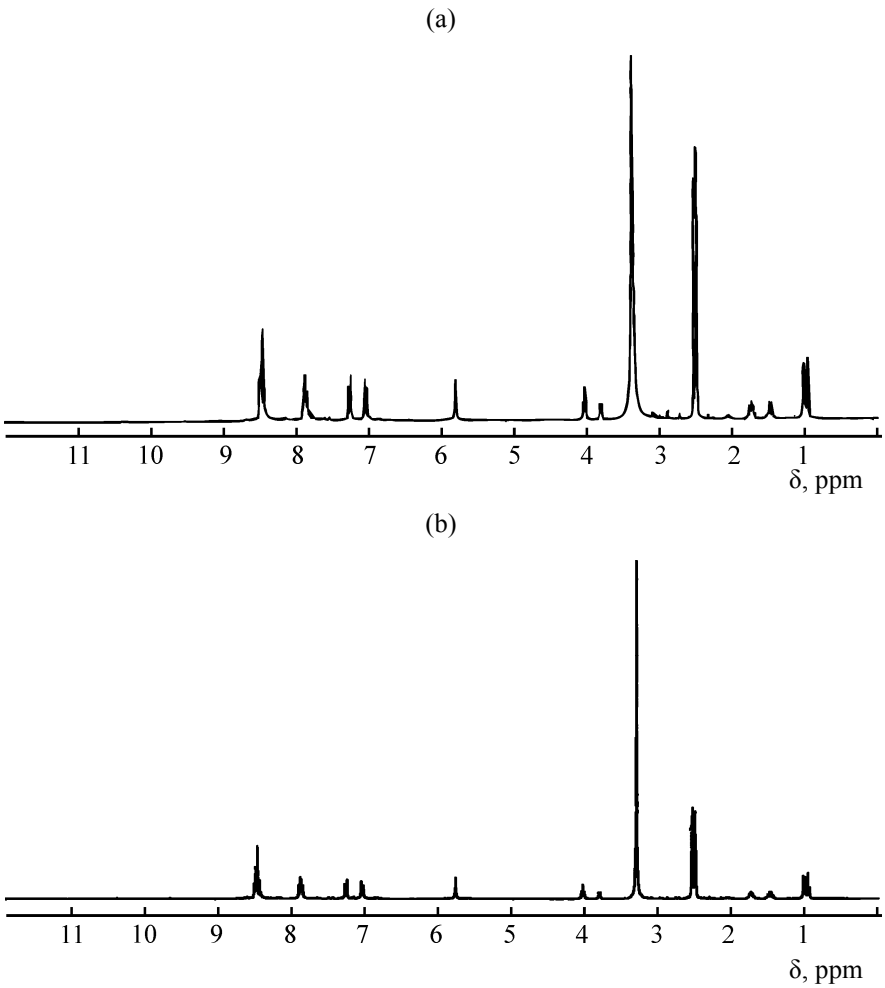

Fig. 2. ^{1}H NMR spectra of (a) **II** and (b) **III** complexes.

assigned to loss of another water molecule (weight loss: observed, 1.4% and calculated, 1.9%). The third step observed at 551 K was accompanied by mass loss (observed, 14.2% and calculated, 14.8%) assigned to loss of (CH_4 + N_2 + 4.5O + 3.5H_2). The fourth step falls in 633 K, accompanied by mass loss (observed, 17.4% and calculated, 17.4%) which is assigned to loss of (CH_2Cl_2 + 2NH_3 + C_2H_2). The fifth step falls in 712 K, accompanied by mass loss (observed, 7.9% and calculated, 8.2%) which is assigned to loss of (CO + HCl + 2H_2). The final step occurs at 799 K, accompanied by mass loss (observed, 12.7 and calculated, 12.5%) which is assigned to loss of (SO_2 + C_2H_4 + 4H_2). The ($NdO_{1.5}$ + 17C) is the final product remains stable up to 1073 K.

To make sure about the proposed formula and structure for the Tb(III) complex, thermo gravimetric (TG) and differential thermo gravimetric (DTG) were carried out for this complex under nitrogen flow. The thermal decomposition for [Tb(GMP)(H_2O)$_4$].Cl_3.H_2O complex occurs in four steps. The first degradation step takes place in the range of 298–346 K and corresponds to the elimination of H_2O molecule (weight loss: observed, 2.0% and calculated, 2.1%). The second step falls in 399 K which is assigned to loss of 3H_2O molecules (observed, 6.0% and calculated, 6.3%). The third step was observed at 501 K (observed, 50.9% and calculated, 51.0%) which is assigned to loss of (6C_2H_2 + SO_2 + 2NH_4Cl + 3C_2H_2 + 2CO + HCl + 0.5H_2O). The final step falls in 798 K, (observed, 7.4% and calculated, 7.3%) which is assigned to loss of (C_2H_4 + 2NH_3). The ($TbO_{1.5}$ + 8C) is the final product remains stable till 1073 K.

The TG curve of [Er(GMP)(H_2O)$_4$]Cl_3·10H_2O complex indicates that the mass change begins at 306 K and continues up to 814 K. The first mass loss

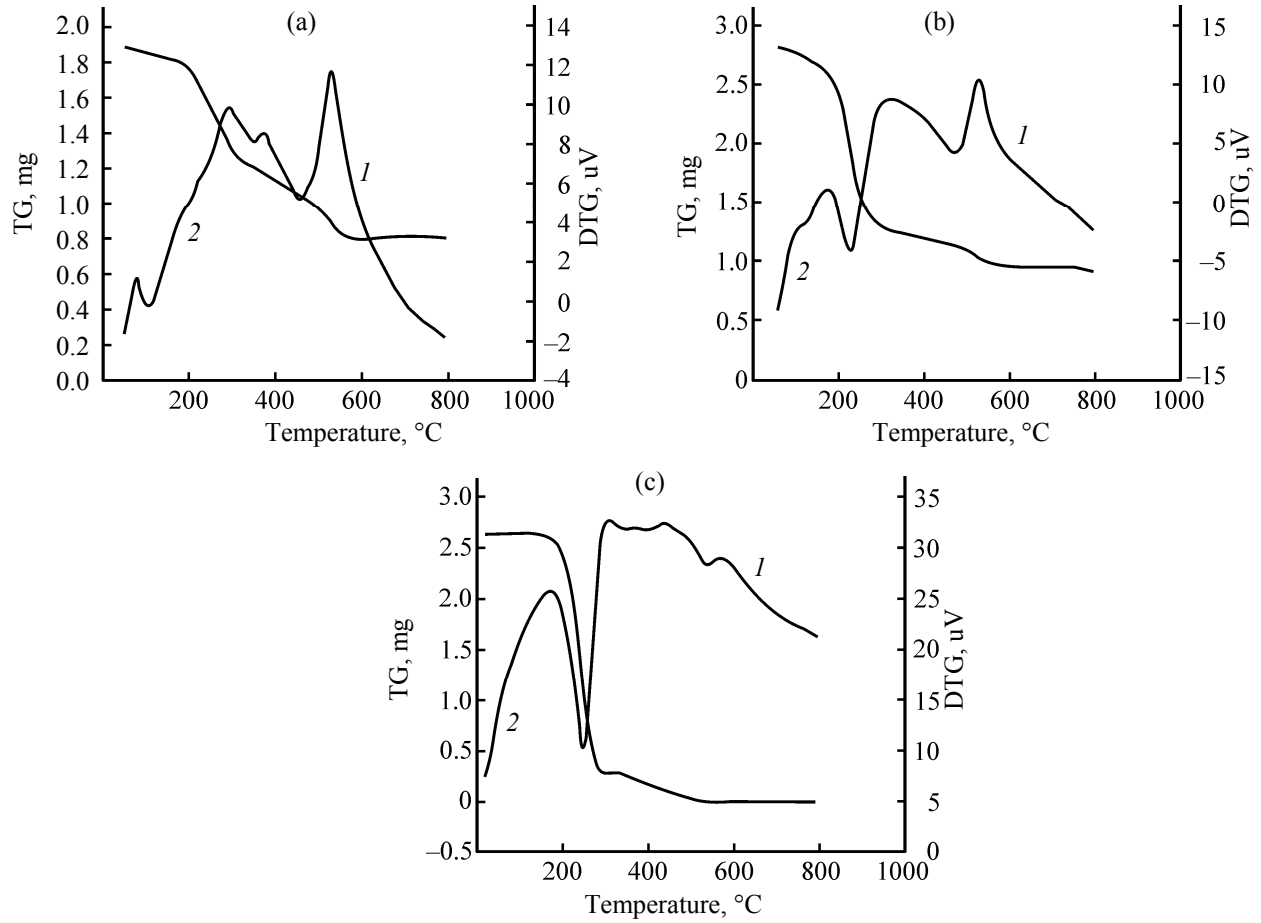

Fig. 3. (*1*) TG and (*2*) DTG curves of complexes: (a) **I**, (b) **II**, and (c) **III**.

corresponds to the liberation of one water molecule (weight loss: observed, 1.3%, calculated, 1.7%). The second decomposition step occurs at 521 K and corresponds to the loss of ($6C_2H_2 + CH_4 + 3NH_4Cl + SO_2 + 5CO + 8.5H_2O + 2H_2 + NH_3$) (observed, 70.7%, calculated, 70.3%). The third decomposition step occurs at 624 K and corresponds to the loss of ($CO + C_2H_4$) (observed, 5.3%, calculated, 5.5%). The final decomposition step occurs at 789 K and corresponds to the loss of (C_2H_4) (observed, 3.1%, calculated, 3.0%). DTG profile shows four endothermic peaks. The final residue at the end of this stage is ($ErO_{1.5} + C$).

Kinetic studies. In recent years there has been increasing interest in determining the rate-dependent parameters of solid-state non-isothermal decomposition reactions by analysis of TG curves [27–32]. Most commonly used methods are the differential method of Freeman and Carroll [26] integral method of Coat and Redfern [27] and the approximation method of Horowitz and Metzger [30]. In the present investigation, the general thermal behaviors of the Glimepiride complexes in terms of stability ranges, peak temperatures and values of kinetic parameters, are shown in (Fig. 4 and Table 5). The kinetic parameters have been evaluated using the Coats-Redfern equation:

$$\int_0^{\alpha} \frac{d\alpha}{(1-\alpha)^n} = \frac{A}{\varphi} \int_{T_1}^{T_2} \exp(-\frac{E^*}{RT})dt. \qquad (1)$$

This equation on integration gives

$$\ln\left[-\frac{\ln(1-\alpha)}{T^2}\right] = -\frac{E^*}{RT} + \ln\left[\frac{AR}{\varphi E^*}\right], \qquad (2)$$

A plot of left-hand side (LHS) against $1/T$ was drawn. E^* is the energy of activation in J mol^{-1} and calculated from the slop and A in (s^{-1}) from the intercept value. The entropy of activation ΔS^* in (J K^{-1} mol^{-1}) was calculated by using the equation:

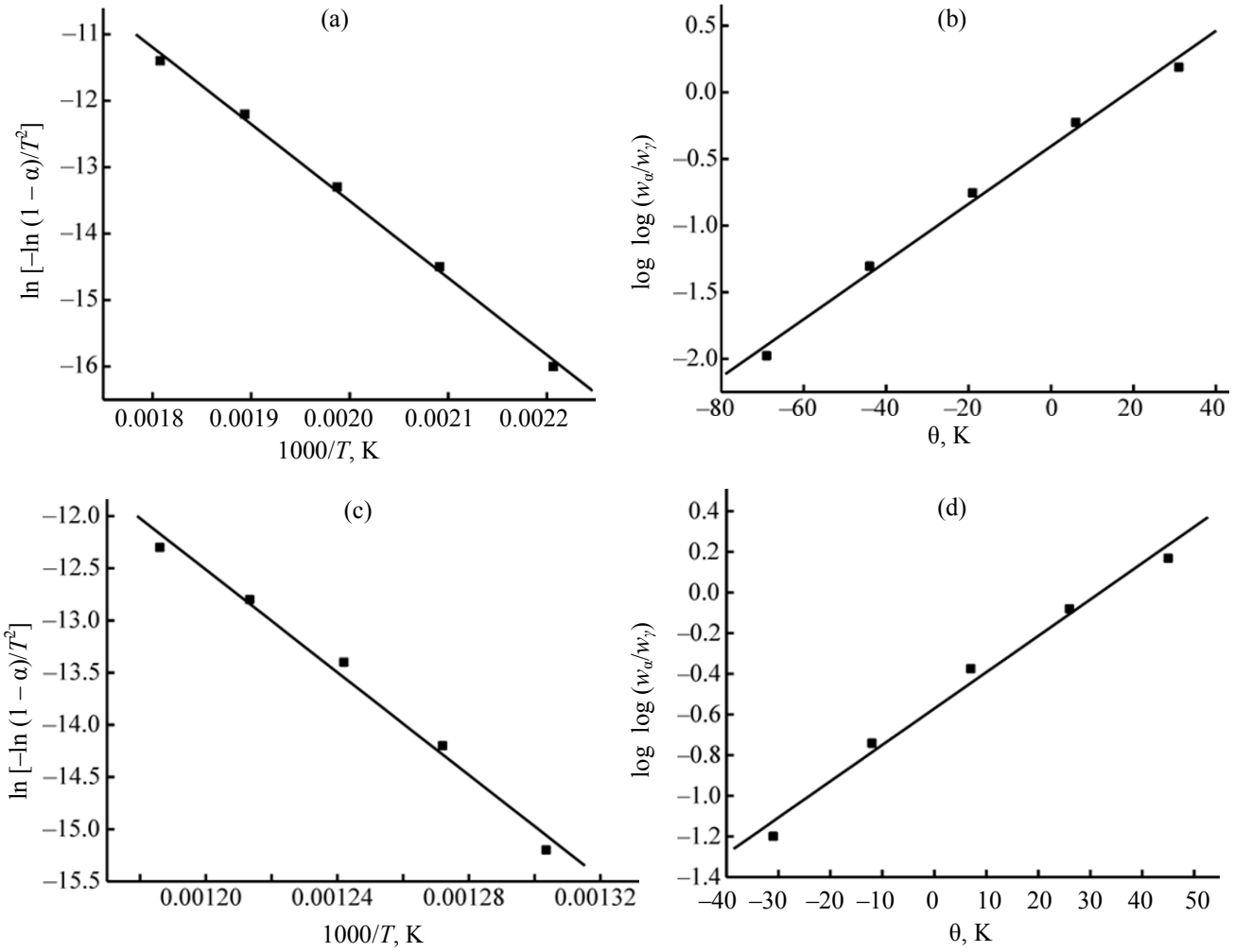

Fig. 4. (a, c) Coat-Redfern (CR) and (b, d) Horowitz and Metzger (HM) curves for Glimepiride complexes: (a, b) **III**, (c, d) **I**.

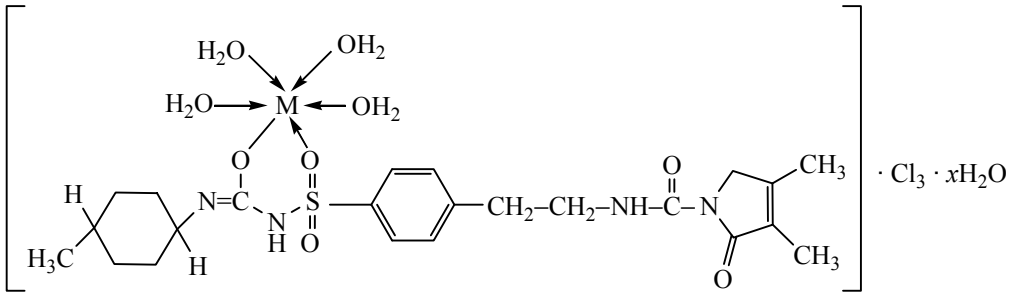

Fig. 5. Mode of chelatation of Glimepiride complexes [where M= Nd(III), Tb(III), and Er(III); x = 1 and 10].

$$\Delta S^* = R\ln (Ah/k_B T_s), \quad (3)$$

where k_B is the Boltzmann constant, h is the Plank's constant and T_s is the DTG peak temperature [33].

The Horowitz-Metzger equation is an illustrative of the approximation methods.

$$\log [\{1 - (1 - \alpha)^{1-n}\}/(1 - n)] = E^*\theta/2.303RT_s^2, \quad n \neq 1. \quad (4)$$

When n = 1, the LHS of Eq. (4) would be log [–log (1 – α)]. For a first-order kinetic process the Horowitz-Metzger equation may be written in the form:

Table 4. Thermal data of Glimepiride and its complexes

Comp. no.	Step	Temperature range, °C	DTG peak, °C	TG weight		Assignments
				calculated	found	
I	1	50–150	74.25	2.1	2.0	H_2O
	2	200–250	224.92	1.9	1.4	H_2O
	3	260–310	278.24	14.8	14.2	$CH_4 + N_2 + 4.5O + 3.5H_2$
	4	335–380	359.90	17.4	17.4	$CH_2Cl_2 + C_2H_2 + 2NH_3$
	5	410–480	439.00	8.2	7.9	$CO + HCl + 2H_2$
	6	500–800	526.29	12.5	12.7	$SO_2 + C_2H_4 + 4H_2$
						$NdO_{1.5} + 17C$
II	1	40–110	73.33	2.0	2.1	H_2O
	2	120–330	125.98	6.0	6.3	$3\ H_2O$
	3	350–550	228.55	50.9	51.0	$6C_2H_2 + SO_2 + 2NH_4Cl + 2CO + HCl + 0.5H_2O$
		550–800	252.00	7.4	7.3	$2CH_2 + 2NH_3$
	4					$TbO_{1.5} + 8C$
III	1	30–150	33.54	1.3	1.7	H_2O
	2	200–300	247.75	70.7	70.3	$6C_2H_2 + CH_4 + 3NH_4Cl + SO_2 + 5CO + 8.5H_2O + 2H_2 +$
	3	330–490	350.38	5.3	5.5	NH_3
	4	500–800	516.46	3.1	3.0	$C_2H_4 + CO$
						C_2H_4
						$ErO_{1.5} + C$

$$\log [\log (w_\alpha / w_\gamma)] = E^*\theta/2.303RT_s^2 - \log 2.303,$$

where $\theta = T - T_s$, $w_\gamma = w_\alpha - w$, w_α = mass loss at the completion of the reaction; w = mass loss up to time t. The plot of log [log (w_α/w_γ)] vs θ was drawn and found to be linear from the slope of which E^* was calculated. The pre-exponential factor, A, was calculated from the equation:

$$E^*/RT_s^2 = A/[\ \varphi \exp(-E^*/RT_s)].$$

The entropy of activation, ΔS^*, was calculated from Eq. (3). The enthalpy activation, ΔH^*, and Gibbs free energy, ΔG^*, were calculated from; $\Delta H^* = E^* - RT$ and $\Delta G^* = \Delta H^* - T\Delta S^*$, respectively.

From the kinetic and thermodynamic data resulted from the TGA curves and listed in Table 5, the following conclusions could be done:

(1) Thermodynamic data obtained with the two methods are in accordance with each other.

(2) The higher values of activation energies of the Glimepiride complexes led to thermal stability of the studied complexes.

(a) (b)

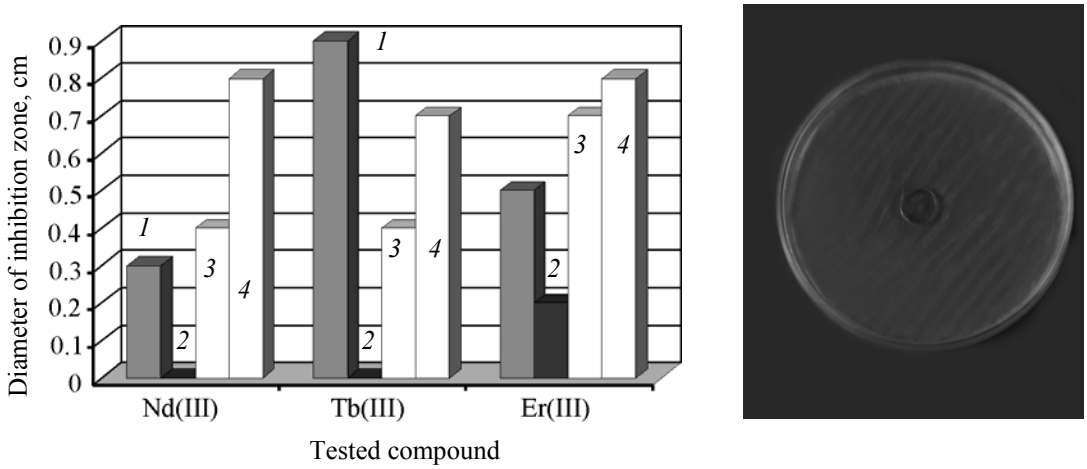

Fig. 6. (a) Microbial test for Glimepiride and its complexes, (b) inhibition of Tb(III) complex against *B. Subtillis*. (*1*) *B. subtilis* (*2*) *E. coli,* (*3*) *Pencillium,* and (*4*) *spergillus.*

Table 5. Thermodynamic parameters of the thermal decomposition of Glimpiride complexes

Comp. no.	Thermodynamic parameters	Methods	
		CR	HM
I	*r*	0.99862	0.99644
	*E**	9.63E+04	1.13E+05
	A	4.51E+07	2.53E+09
	Δ*S**	–1.03E+02	–6.96E+01
	Δ*H**	9.20E+04	1.09E+05
	Δ*G**	1.46E+05	1.45E+05
II	*r*	0.99364	0.99256
	*E**	2.05E+05	2.18E+05
	A	1.49E+11	1.93E+12
	Δ*S**	–3.92E+01	–1.79E+01
	Δ*H**	1.98E+05	2.11E+05
	Δ*G**	2.29E+05	2.26E+05
III	*r*	0.99709	0.99629
	*E**	2.57E+05	2.76E+05
	A	6.09E+14	1.43E+16
	Δ*S**	2.99E+01	5.61E+01
	Δ*H**	2.50E+05	2.69E+05
	Δ*G**	2.26E+05	2.24E+05

Table 6. Antimicrobial activity of Glimpiride and its complexes

Tested compounds	Diameter of inhibition zone, cm			
	B. subtilis	*E. coli*	*P. rotatum*	*A. nigar*
I	0.3	0	0.4	0.8
II	0.9	0	0.4	0.7
III	0.5	0.2	0.7	0.8

(3) The correlation coefficients of the Arrhenius plots of the thermal decomposition steps were found to lie in the range 0.9820 to 0.9996, showing a good fit with linear function.

(4) It is clear that the thermal decomposition process of all Glimepiride complexes is non-spontaneous, i.e., the complexes are thermally stable.

Structure of the glimepiride complexes. Finally on the basis of the above studies, the suggested structures of the Glimepiride complexes can be represented as in Fig. 5.

Antimicrobial activity. The results of the antimicrobial tests are given in Table 6 and in Fig. 6. Tb(III)/GMP complex is active against *B. subtilus*, while Nd(III)/GMP and Er(III)/GMP complexes showed activity against *Aspergillus nigar*.

REFERENCES

1. Nartindale. *The Complete Drug Reference*, London: Pharmaceutical Press, 32 ed, 1999, p. 320.
2. *British Pharmacopeia,* United Kingdom, The Stationery Office, 1998, pp. 637–638.
3. Roask, C., *J. Diabetes Complicat*., 2002, vol. 16, pp. 123–132.
4. Muller, G. and Wied, S., *Diabetes,* 1993, vol. 42, pp. 1852–1867.
5. Haupt, A., Kausch, C., Dahl, D., Bachmann, O., Stumvoll, M., Haring, H.U., . and Matthaei, S., *Diabetes Care*, 2002, vol. 25, pp. 2129–2132.
6. Rosenstock, J., Schneider, J., Samols, E., and Mushmore, D.B., *Diabetes Care,* 1996, vol. 19, pp. 1194–1199.
7. Rosskamp, R., Wernicke-Panten, K., and Draeger, E., *Diabetes Res. Clin. Pract.,* 1996, vol. 31, pp. 33–42.
8. Inukai, K., Watanabe, M. Nakashima, Y., Sawa, T., Takata, N., Tanaka, M,. Kashiwabara, H., Yokota, K., Suzuki, M., Kurihara, T., Awata, T., and Katayama, S., *Diabetes Res. Clin. Pract.* (in press).
9. Clark, H.E. and Mattews, D.R., *Horm. Metab. Res.,* 1996, vol. 28, pp. 445–450.
10. Muller, G., *Mol. Med*., 2000, 6, pp. 907–933.
11. Draeger, E., *Diabet. Res*. *Clin. Prac.,* 1995, vol. 28 (suppl.) pp. 139-146.
12. Babu, R.J. and Pandit, J.K., *Drug Dev. Ind. Pharm.,* 1999, vol. 25, pp. 1215–1219.
13. Iqbal, S.A., Sibi, J., and Jacob, G., *Oriental J. Chem.,* 2011, vol. 27, no. 2, pp. 731–735.
14. Shirse, P., *IJRAP,* 2012, vol. 3, no. 3, pp. 465–470.
15. Gupta, R, Saxena, R.K., Chatarvedi, P., and Virdi, J.S., *J. Appl. Bacteriol.,* 1995, 87, p. 378.
16. Geary, W.J., *Coord. Chem. Rev.,* 1971, vol. 7 p. 81.
17. Houte, S.E.I. and Sayed Ali, M.E.I., *J. Therm. Anal.,* 1991, vol. 37, p. 907.
18. Iqbal, S.A, *Bull. Pure Appl. Sci.*, 1984, vol. 3C, no. 2, pp. 85–87.
19. Cotton, F.A, *Int. Sci. Pub. Ed.*, 1960.
20. Scott, A., *Standard Methods of Chemical Analysis*, Van Nostrand, 1960, p. 634.
21. Houte, S.E.I., and Sayed Ali, M.E.I., *J. Therm. Anal.*, 1991, vol. 37, p. 907.

22. Sharma, S., Iqbal, S. A. and Bhattacharya, M., *Orient. J. Chem;* 2009, vol. 25, no. 4, pp. 1101–1104.
23. Siddiqui, A., Iqbal, S.A., and Qureshi, S., *Orient. J. Chem.,* 2004, vol. 20: p. 655.
24. Budhani, P., Iqbal, S.A., and Malik, S., *Orient. J. Chem.,* 2005, vol. 21, p. 147.
25. Iqbal, S.A., Jacob, G., and Malik, S., *Orient. J. Chem.,* 1998, vol. 14, p. 116.
26. Freeman, E.S. and Carroll, B., *J. Phys. Chem.,* 1958, vol. 62, p. 394.
27. Coats, A.W. and Redfern, J.P, *Nature,* 1994, vol. 201, pp. 68–69.
28. Ozawa, T., *Bull. Chem. Soc. J.* 1965, 38 p. 1881.
29. Wendlandt, W.W., *Thermal Methods of Analysis*, New York: Wiley, 1974.
30. Horowitz, H.W. and Metzger, G., *Anal. Chem.,* 1963, vol. 35, p. 1464.
31. Flynn, J.H. and Wall, L.A., *Polym. Lett.,* 1966, vol. 4, p. 323.
32. Kofstad, P., *Nature,* 1957, vol. 179, p. 1362.
33. Flynn, J.H.F and Wall, L.A., *J. Res. Natl. Bur. Stand*., 1996, vol. 70A, p. 487.